Growth and Evolution of Perylene Thin Films on Cu(110)

Q. Chen,* A. J. McDowall, and N. V. Richardson

School of Chemistry and Ultrafast Photonics Collaboration, University of St. Andrews, North Haugh, St. Andrews, Fife KY16 9ST, UK

Received April 8, 2003. Revised Manuscript Received July 30, 2003

The growth of ordered perylene structures on a Cu(110) surface has been studied by low-energy electron diffraction and scanning tunneling microscopy. Submonolayer STM images show a centered structure with the molecular plane parallel to the substrate. A sequence of STM images indicates molecular diffusion even at room temperature. The monolayer-covered surface shows a c(8 × 4) periodicity, which transfers into a $\begin{pmatrix} 3 & 1 \\ -2 & 3 \end{pmatrix}$ structure on annealing at 450 K. On further increasing the surface coverage at room temperature, on top of the c(8 × 4) structure, an ordered multilayer structure grows with molecular rows aligned along the ⟨110⟩ azimuth.

1. Introduction

A limitation in the use of organic materials as semiconductors in light-emitting devices is the low conductivity or the low mobility of the charge carrier. The development and control of the ordering of organic semiconductor systems is currently of considerable interest as a means of optimizing the carrier mobilities.[1−4] The optical and electronic properties of these crystalline organic films depend crucially on their orientation and the long range ordering,[4−9] which, in turn, determines their suitability for molecular electronic devices such as FETs, LEDs[1,10] etc. It has been suggested[11,12] that improved internal ordering of the organic thin film could enhance field-effect carrier mobilities, together with increased electrical conductivity and reduced activation energy for electrical conduction.

Planar aromatic hydrocarbons typically have a shallow and broad intermolecular interaction potential energy surface dominated by van der Waals interactions. Thus, the molecule−substrate interaction could play a significant role in determining the commensurability and subsequent 3D crystalline structure. Recently,[13] we have shown that a novel, well-ordered perylene multilayer structure, shown in Figure 1a, can be formed on clean Cu(110) surfaces. Figure 1b shows the structure of the perylene molecule, and Figure 1c shows the STM image of a small area marked in Figure 1a. The multilayer has a centered orthorhombic structure with dimensions $a = 20.7$ Å, $b = 19.3$ Å, $c = 3.4$ Å, and $\beta = 90°$. It is commensurate along the substrate ⟨110⟩ direction, but not along the ⟨001⟩ azimuth. Flat-lying molecules form one-dimensional chains in the ⟨110⟩ azimuth with a 90° azimuthal rotation between neighboring molecules in the chain; whereas along the ⟨001⟩ azimuth, the molecular chains keep a large separation of 19.3 Å, incommensurate with respect to the copper lattice. This distance is also much larger than the molecular dimensions. In the 3D structure, this structure is stabilized through an ABA layer arrangement while alternate layers are π-stacked. However, if the monolayer were to have the same structure as a single plane of the molecules, the surface coverage would be very low, at only 50% of the expected saturation coverage based on the molecular dimensions. Therefore, several questions remain. What is the monolayer structure and how is it related to the substrate lattice? How does this evolve into the novel multilayer structure?

In this paper, we present the results of STM and LEED observations of submonolayer and monolayer structures, which appear to be different from, but in certain cases correlated with, the multilayer structure. The evolution of the multilayer from the monolayer is also presented.

2. Experimental Section

Experiments were carried out in two different UHV instruments, base pressure ∼1×10^{-10} mbar, equipped with low energy electron diffraction (LEED) and either vt-STM (Omicron) or high-resolution electron energy loss spectroscopy (HREELS) (VSW HIB 1000 double pass spectrometer). Both systems have a Hiden quadrupole mass spectrometer to monitor the molecular deposition. The Cu(110) crystals were cut and polished mechanically, and for STM experiments electrochemically, to a mirror finish before insertion into UHV

* Corresponding author. Fax: (+44)1334-467285. E-mail: qc@st-andrews.ac.uk.

(1) Ozaki, H. *J. Chem. Phys.* **2000**, *113*, 6361.
(2) Morozov, A. O.; Kampen, T. U.; Zahn, D. R. T. *Surf. Sci.* **2000**, *446*, 193.
(3) Müller, E.; Ziegler, C. *J. Mater. Chem.* **2000**, *10*, 47.
(4) Böhler, A.; Urbach, P.; Schöbel, J.; Dirr, S.; Johannes, H. H.; Wiese, S.; Ammermann, D.; Kowalsky, W. *Physica E* **1998**, *2*, 562.
(5) Toda, Y.; Yanagi, H. *Appl. Phys. Lett.* **1996**, *69*, 2315.
(6) Cho, K. J.; Shim, H. K.; Kim, Y. I. *Synth. Met.* **2001**, *117*, 153.
(7) Colle, M.; Tsutsui, T. *Synth. Met.* **2000**, *111*, 95.
(8) Feng, W.; Fujii, A.; Lee, S.; Wu, H.; Yoshino, K. *J. Appl. Phys.* **2000**, *88*, 7120.
(9) Gerasimova, N. B.; Komolov, A. S.; Aliaev, Y. G.; Sidorenko, A. G. *Phys. Low-Dimens. Struct.* **2001**, *1−2*, 119.
(10) Yamaguchi, T. *J. Phys. Soc. Japan* **1999**, *68*, 1321.
(11) Salih, A. J.; Lau, S. P.; Marshall, J. M.; Maud, J. M.; Bowen, W. R.; Hilal, N.; Lovitt, R. W.; Williams, P. M. *Appl. Phys. Lett.* **1996**, *69*, 2231.
(12) Karl, N.; Marktanner, J. *Mol. Cryst. Liquid Cryst.* **2001**, *355*, 149.
(13) Chen, Q.; Rada, T.; McDowall, A.; Richardson, N. V. *Chem. Mater.* **2002**, *14*, 743.

10.1021/cm031067z CCC: $25.00
Published on Web 09/09/2003

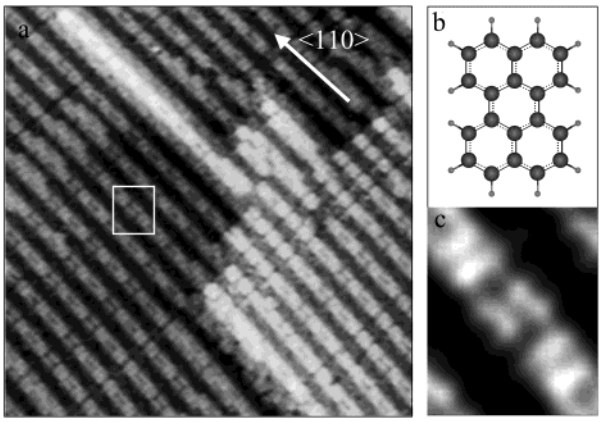

Figure 1. (a) STM image (30 nm × 30 nm, $V = 0.01$ V, $I = 0.47$ nA) of ordered multilayer of perylene on a Cu(110) surface. (b) The chemical structure of the perylene molecule. (c) An enlarged image of an area marked in (a).

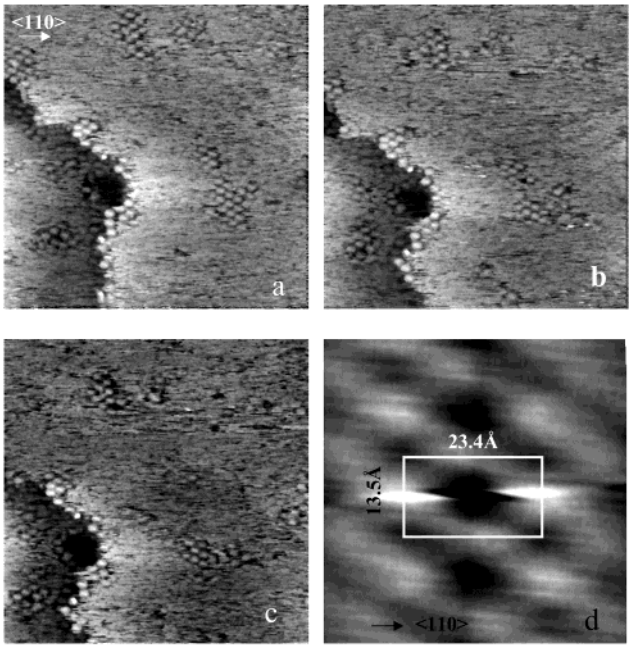

Figure 2. (a−c) A sequence of STM images (43 nm × 43 nm, $V = 0.01$ V, $I = 0.13$ nA, time interval = 5 min) of the same area show the ordering and diffusion of low coverage perylene. (d) The autocorrelation function from image (a). The periodicity is indicated.

where they were cleaned by standard Ar^+ bombardment (typically, 500 eV, 30 μA cm^{-2}) and annealing (773 K) procedures until a clean surface was obtained, characterized by sharp (1 × 1) LEED patterns and large flat terraces in STM.

Perylene (Sigma, 99%) was degassed for 3 h at 333 K before dosing. The doser consists of a glass tube with heating wire and thermocouple sensor, so the dosing temperature is well controlled and the reproducibility is ensured. The same doser was used in both systems. Perylene was dosed at 433 K, corresponding to a dosing pressure of 1×10^{-9} mbar, with the substrate at room temperature.

3. Results and Discussion

The submonolayer coverage was achieved by dosing for 1 min. Figure 2a shows a typical STM image of the surface at low coverage (~0.1 mL). The sample was mounted in such an orientation that the ⟨110⟩ azimuth was roughly in the horizontal direction and the ⟨001⟩ azimuth was in the vertical direction. The molecules in small islands seem to be in a centered structure, with their longer axis preferentially orientated parallel to the ⟨110⟩ direction. Figure 2b and c shows sequential STM images of the same area separated by 5 min. The images indicate an equilibrium between molecules present in islands and as a 2D gas. Diffusion is sufficiently rapid, possibly tip enhanced, that islands appear, disappear, and change shape on a time scale of a few minutes, corresponding to a small diffusion barrier to molecular motion. No isolated single molecule can be imaged because of its higher mobility with a diffusion barrier less than the thermal energy at room temperature, 25 meV.

At this stage, no new LEED pattern was observed. However, the 2D autocorrelation function of the STM image, shown in Figure 2d, does show evidence of a periodic structure in the islands. The unit cell is centered rectangularly with a length of 13.5 Å in the ⟨001⟩ direction and 23.4 Å in the ⟨110⟩ direction. Without another known periodicity in the same STM image or a diffraction pattern, it is difficult to calibrate the drift of the piezo. However, the typical angular and lateral drift of our STM piezo gives rise to a possible error of up to ±20% in the unit cell dimensions and enclosed angle.

Dosing perylene for longer, 10 min, at the same dosing temperature, a saturated monolayer is formed. Figure 3 shows the STM image (a), its autocorrelation function (b), and the LEED pattern (c) of the surface. Again, the STM image shows a centered structure. The FFT of the image (inset to Figure 3a) shows four distinctive spots with an enclosed angle of 71 ± 2°. The real space periodicity can be clearly identified in the autocorrelation image (Figure 3b). The unit cell vectors are ±35° to the ⟨110⟩ direction and have a length of 12.5 Å, corresponding to the (4, ±2) vectors and a c(8 × 4) periodicity. The c(8 × 4) rectangular unit cell, which has dimensions of 20.5 Å along ⟨110⟩ and 14.4 Å along ⟨001⟩, suggests that, within experimental error, this is the same as the periodicity observed in the islands at low coverage. The idealized c(8 × 4) unit cell contains two equivalent perylene molecules. However, the STM image does not give a clear indication of the molecular orientation and it may be that there is considerable disorder in the azimuthal orientation although each molecule lies on the c(8 × 4) lattice. On average each molecule occupies 147.3 $Å^2$ corresponding to 16 Cu atoms. This area is much larger than the molecular "footprint", ca. 100 $Å^2$, suggesting a rather widely spaced structure linked to the azimuthal orientational disorder. The LEED pattern confirms the c(8 × 4) periodicity but the spots are rather broad indicating small domains perhaps also, indirectly linked to the azimuthal disorder. Three possible models of (8 × 4) structure are shown in Figure 4. A unit cell containing two structurally inequivalent molecules, strictly a p(8 × 4) unit cell, in which the two molecules are rotated by a 90° rotation is shown in Figure 4C. The difference between these models is only in the molecular orientation. The closest H···H distances between adjacent molecules are similar for these models, at 3.38 Å for model A, 3.48 Å for model B, and 3.37 Å for model C. DFT ab initio calculations of the interaction energy between a pair of molecules in the different models have been carried out using fully

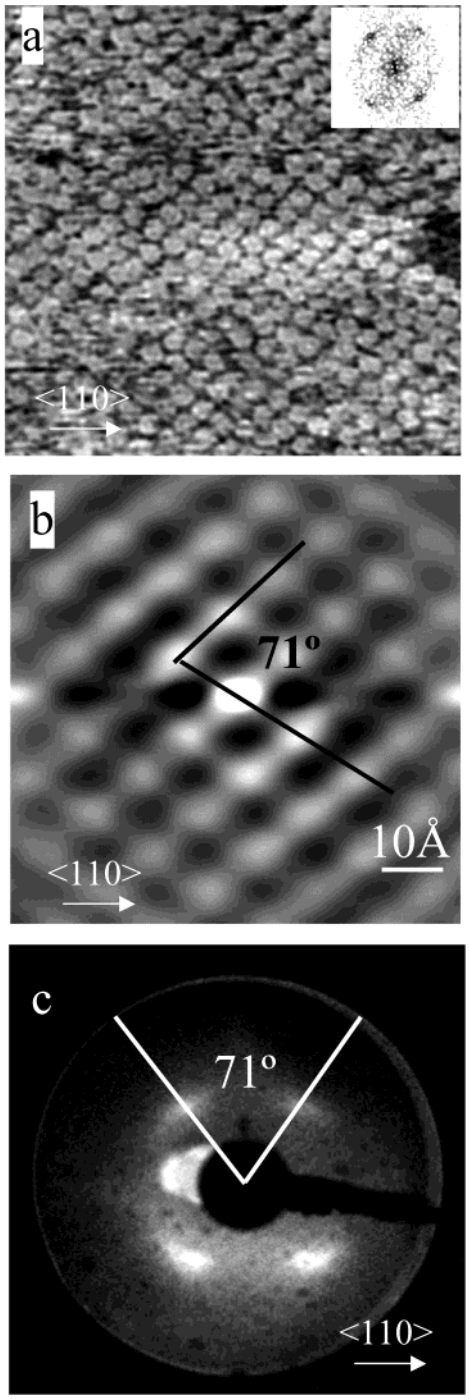

Figure 3. (a) STM image (20 nm × 20 nm, $V = 0.01$ V, $I = 0.3$ nA) of monolayer coverage perylene on Cu(110). (b) Autocorrelation function of the image in (a). (c) LEED pattern (12 eV) of the same surface with a diffuse c(8 × 4) periodicity.

optimized free molecular geometry based on B3LYP[14] methods and a 6−31 g* basis set with Gaussian 98W.[15] The calculations indicate weak but attractive interactions between the pairs of molecules, which are 0.639, 0.807, and 0.691 kJ/mol for models A, B, and C, respectively. Therefore the energetics would seem to favor the longer molecular axis being aligned with the ⟨001⟩ azimuth, as shown in Figure 4B. The energetic similarity of these structures may be the source of the azimuthal disorder and small domain size. Domain

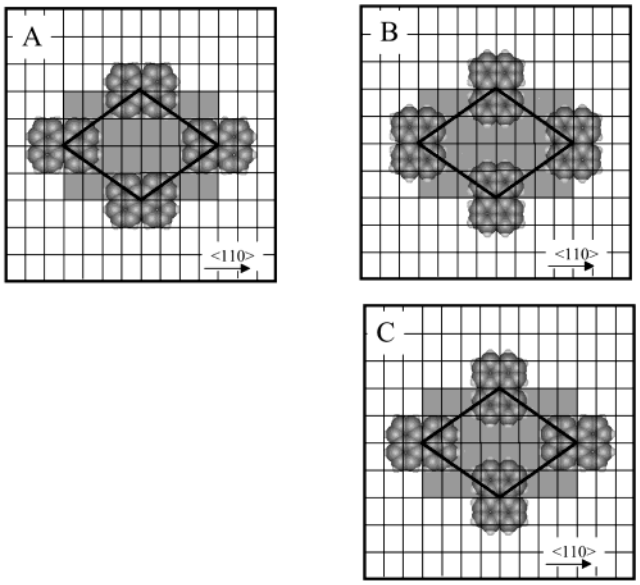

Figure 4. Three proposed models of (8 × 4) structure with different molecular orientation.

boundaries seem to have a higher local density of molecules on the basis of the STM images, such as that shown in Figure 3a.

Following deposition at room temperature, annealing the weakly ordered c(8 × 4) structure at 450 K results in a more closely packed, ordered structure. In comparison with the c(8 × 4), the LEED pattern shown in Figure 5a is relatively complex with none of the overlayer lattice vectors aligned along the high-symmetry axes. The real space unit cell can be described in a matrix notation $\begin{pmatrix} 3 & 1 \\ -2 & 3 \end{pmatrix}$, where each row represents one of the real space unit cell lattice vectors. Conventionally, the first integer in each row refers to the ⟨110⟩ direction of the copper surface, in units of the interatomic spacing $d_{Cu-Cu} = 2.55$ Å, and the second integer refers to the ⟨001⟩ direction with units of $\sqrt{2}d_{Cu-Cu} = 3.61$ Å. The (3, 1) vector is 8.46 Å long and oriented 25.26° respect to the ⟨110⟩ direction, while the vector (−2, 3) is 11.97 Å long and aligned 64.79° respect to ⟨110⟩. Considering neither of the defining vectors is aligned with the high-symmetry direction of substrate unit cell, two domains are implied, related by reflection across the ⟨110⟩ direction (or the ⟨001⟩ direction). In matrix notation, the reflectional domain can be defined as $\begin{pmatrix} -3 & 1 \\ 2 & 3 \end{pmatrix}$. The reciprocal lattice vectors and higher order diffraction spots, within the first-order substrate diffraction pattern, are illustrated in Figure 5b and the real space unit cells are shown in Figure 5c. In Figure 5b, the solid and dashed meshes correspond to the two domains, and LEED spots can be found at the intersections in each mesh. The rectangular unit cell is 11 times larger than

(14) Becke, A. D. *Phys. Rev. a* **1988**, *38*, 3098.

(15) Frisch, M. J.; Trucks, G. W.; Schlegel, H. B.; Scuseria, G. E.; Robb, M. A.; Cheeseman, J. R.; Zakrzewski, V. G.; Montgomery, J. A.; Stratmann, R. E.; Burant, J. C.; Dapprich, S.; Millam, J. M.; Daniels, A. D.; Kudin, K. N.; Strain, M. C.; Farkas, O.; Tomasi, J.; Barone, V.; Cossi, M.; Cammi, R.; B. Mennucci; Pomelli, C.; Adamo, C.; Clifford, S.; Ochterski, J.; G. A. Petersson; Ayala, P. Y.; Cui, Q.; Morokuma, K.; Malick, D. K.; Rabuck, A. D.; Raghavachari, K.; Foresman, J. B.; Cioslowski, J.; Ortiz, J. V.; Stefanov, B. B.; Liu, G.; Liashenko, A.; Piskorz, P.; Komaromi, I.; Gomperts, R.; Martin, R. L.; Fox, D. J.; Keith, T.; Al-Laham, M. A.; Peng, C. Y.; Nanayakkara, A.; Gonzalez, C.; Challacombe, M.; Gill, P. M. W.; Johnson, B. G.; Chen, W.; Wong, M. W.; Andres, J. L.; Head-Gordon, M.; Replogle, E. S.; Pople, J. A. *Gaussian 98W*; Revision A.7 ed.; Gaussian, Inc.: Pittsburgh, PA, 1998.

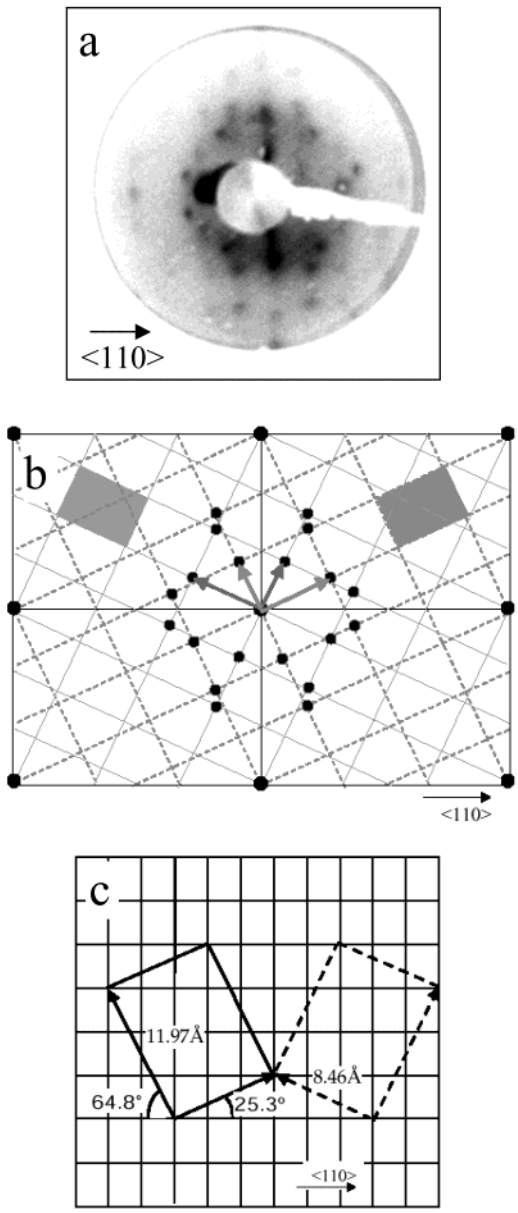

Figure 5. (a) LEED pattern of $\begin{pmatrix} 3 & 1 \\ -2 & 3 \end{pmatrix}$ periodicity, recorded at 17 eV. (b) The reconstructed $\begin{pmatrix} 3 & 1 \\ -2 & 3 \end{pmatrix}$ shows the reciprocal lattice vectors and higher order diffraction spots. (c) Real space unit cells.

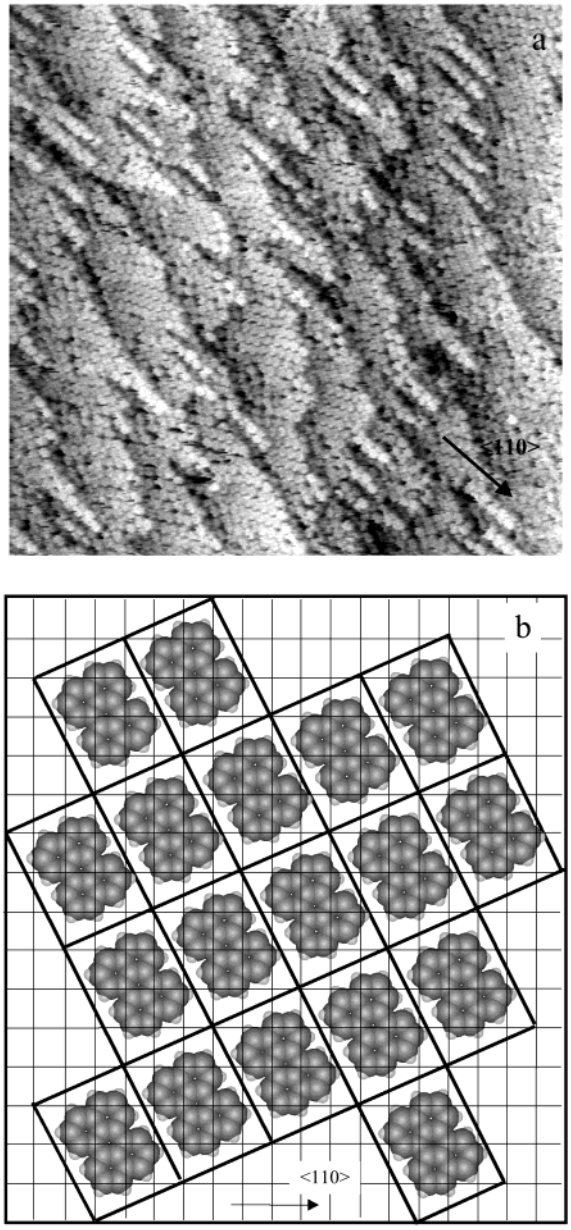

Figure 6. (a) STM image (60 nm × 60 nm, $V = -0.11$ V, $I = 1.83$ nA) of annealed surface with a $\begin{pmatrix} 3 & 1 \\ -2 & 3 \end{pmatrix}$ periodicity. (b) Real space model of $\begin{pmatrix} 3 & 1 \\ -2 & 3 \end{pmatrix}$ structure.

the underlying substrate unit cell, with an area of 101.3 Å^2, which is very close to the area of a flat-lying molecule, ca. 100 Å^2. The length of the sides of the unit cell also corresponds closely to those of the molecule. Therefore, each unit cell can contain only one flat-lying molecule. Compared with the c(8 × 4) structure, the density of molecular packing is increased by 45%. The corresponding STM image and a possible structural model for this annealed surface are shown in Figure 6a and b, respectively. The high-symmetry axes of the perylene molecule are no longer aligned along the high-symmetry axes of the substrate, but the closest packing of the flat-lying perylene molecules in a commensurate structure on the Cu(110) surface is achieved. The minimum H···H distance is 2.2 Å and the improved packing is achieved by interdigitation of the C−H bonds on adjacent molecules.

On the edges of some of the $\begin{pmatrix} 3 & 1 \\ -2 & 3 \end{pmatrix}$ terraces, short rows of molecules grow onto the lower terraces aligned along the ⟨110⟩ azimuth (Figure 6a). Although the ordering of molecules within the rows is not perfect, it is recognizable that the molecular structure within these short rows is the same as that previously observed in the multilayer structure, Figure 1. There are extra features in the electron diffraction pattern, running along the ⟨001⟩ azimuth, which could be contributed from these rows of molecules. In this multilayer structure, we expect relatively strong in-plane intermolecular interaction along the ⟨110⟩ azimuth; whereas along the ⟨001⟩ azimuth, due to the large in-plane space between adjacent rows, intermolecular interactions are limited. However, the ability of the ordered multilayer to grow on this closely packed surface is limited. Searching on different areas of the surface, no molecular rows with substantial length could be found. Meanwhile, no mo-

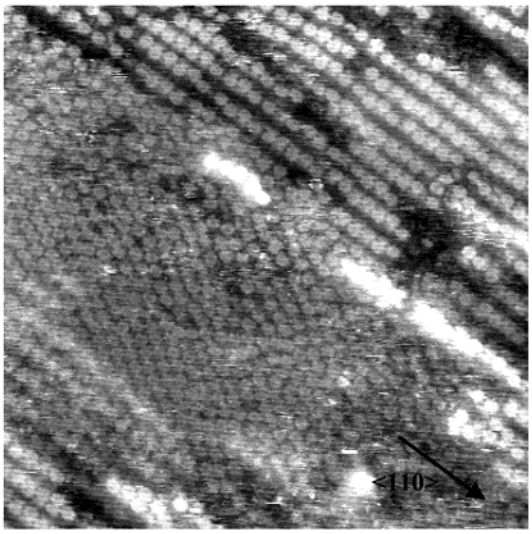

Figure 7. STM image (48 nm × 48 nm, $V = -0.02$ V, $I = 0.73$ nA) with both molecular rows and the c(8 × 4) structure.

lecular rows of this type can be found in the $\begin{pmatrix} 3 & 1 \\ -2 & 3 \end{pmatrix}$ terraces. Also, the (8, 0) vector, the commensurate vector of the multilayer, is not compatible with the $\begin{pmatrix} 3 & 1 \\ -2 & 3 \end{pmatrix}$ periodicity. It is therefore reasonable to assume that the close packed $\begin{pmatrix} 3 & 1 \\ -2 & 3 \end{pmatrix}$ structure is not the monolayer underneath the ordered multilayer.

Further increase deposition on the unannealed surface increases the number and length of the molecular rows, and the structure begins to resemble more closely that of the multilayer. The STM image, Figure 7, shows a surface with both c(8 × 4) and molecular rows. Without annealing, the closely packed $\begin{pmatrix} 3 & 1 \\ -2 & 3 \end{pmatrix}$ periodicity cannot be formed. Therefore it seems likely that molecular rows, aligned along the ⟨110⟩ azimuth, lie above the molecules in the c(8 × 4) domain, i.e., it is likely that the molecular row is formed epitaxially on top of the c(8 × 4) structure. This molecular row, as a part of the centered orthorhombic crystal, is only commensurate with 8-fold periodicity in the ⟨110⟩ azimuth. The coincidence between this 8-fold periodicity and the c(8 × 4) periodicity implies that two structures are compatible at least along one of the unit cell vectors. Figure 8 shows proposed models for both c(8 × 4) and molecular row, multilayer structures. Although the multilayer is incommensurate along the ⟨001⟩ azimuth, it has a periodicity of 19.3 Å, which is about 5.3 times that of the substrate periodicity (3.61 Å). The evolution of the incommensurate multilayer periodicity from the c(8 × 4) will require a lateral relaxation along the ⟨001⟩ azimuth from the 4-fold to 5.3-fold periodicity, which may be energetically compensated by the efficient interlayer interactions. Growing on top of the c(8 × 4) structure, the interaction between alternate planes, i.e. 1, 3, 5 and 2, 4, 6, etc., stabilizes the frame of the 8-fold periodicity in the molecular rows while the incommensurate separation along ⟨100⟩ allows adjacent planes to have a spacing of only 1.7 Å. In turn, this corresponds to alternate planes, and molecules in these planes having a separation of 3.4 Å. This distance is typical of $\pi-\pi$ interactions between aromatic species and indeed is very similar to the basal plane separation of graphite. We consider, therefore, that the stability of the novel structure found for perylene on Cu(110) [13] derives, at least in part, from such favorable $\pi-\pi$ interactions. However, it remains an open question as to whether the first monolayer retains its c(8 × 4) structure on growth of the multilayer or whether it is also reconstructed into the 1D commensurate structure of the multilayer.

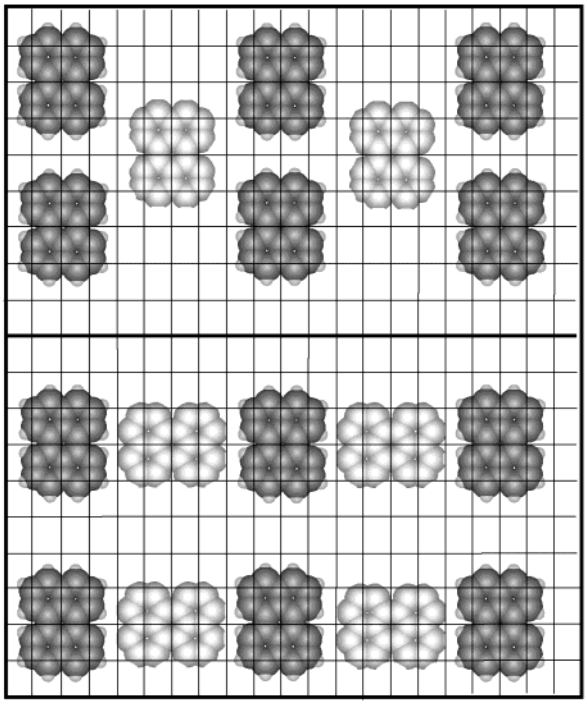

Figure 8. Models of both molecular rows (the lower part) and the c(8 × 4) structure (the upper part). The darker colored molecules represent the common part of these two structures.

Summary

We have shown the coverage-dependent evolution of perylene order structures on Cu(110) surface. At submonolayer, the molecule forms small islands of centered structure with the molecular plane parallel to the substrate. At higher surface coverage, a c(8 × 4) structure, containing two molecules per unit cell, is formed. Annealing this surface forms a closely packed $\begin{pmatrix} 3 & 1 \\ -2 & 3 \end{pmatrix}$ structure, whereas with increasing coverage, ordered multilayer growth is initiated on top of the c(8 × 4) structure. The structural aspect of the epitaxy growth of ordered multilayer is discussed.

CM031067Z